

Improving Color Reproduction Accuracy on Cameras

Hakki Can Karaimer Michael S. Brown
York University, Toronto
{karaimer, mbrown}@eecs.yorku.ca

Abstract

One of the key operations performed on a digital camera is to map the sensor-specific color space to a standard perceptual color space. This procedure involves the application of a white-balance correction followed by a color space transform. The current approach for this colorimetric mapping is based on an interpolation of pre-calibrated color space transforms computed for two fixed illuminations (i.e., two white-balance settings). Images captured under different illuminations are subject to less color accuracy due to the use of this interpolation process. In this paper, we discuss the limitations of the current colorimetric mapping approach and propose two methods that are able to improve color accuracy. We evaluate our approach on seven different cameras and show improvements of up to 30% (DSLR cameras) and 59% (mobile phone cameras) in terms of color reproduction error.

1. Introduction

Digital cameras have a number of processing steps that convert the camera's raw RGB responses to standard RGB outputs. One of the most critical steps in this processing chain is the mapping from the sensor-specific color space to a standard perceptual color space based on CIE XYZ. This conversion involves two steps: (1) a white-balance correction that attempts to remove the effects of scene illumination and (2) a color space transform (CST) that maps the white-balanced raw color values to a perceptual color space. These combined steps allow the camera act as a color reproduction, or colorimetric, device.

The colorimetric mapping procedure currently used on cameras involves pre-computing two CSTs that correspond to two fixed illuminations. The calibration needed to compute these CSTs is performed in the factory and the transform parameters are part of the camera's firmware. The illuminations that correspond to these calibrated CSTs are selected to be "far apart" in terms of correlated color temperature so that they represent sufficiently different illuminations. When an image is captured that is not one of the

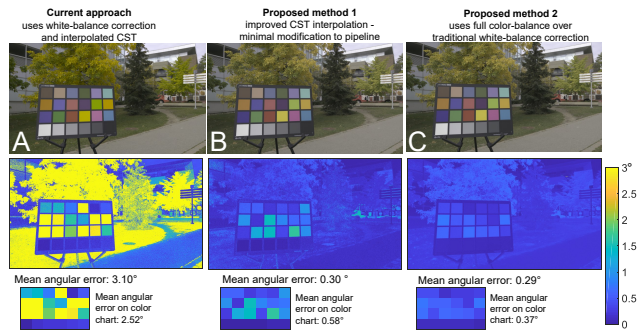


Figure 1: (A) Angular color reproduction error using the current method based on white balance and CST interpolation using two pre-calibrated illuminations. (B) Improvements by our first method using white balance and CST interpolation with three pre-calibrated illuminations. (C) Improvements by our second method using a full color balance and a fixed CST.

two illuminations, an image-specific CST is interpolated by linearly blending the two pre-calibrated CSTs. This reliance on an interpolated CST can result in lower overall perceptual color reproduction accuracy as shown in Figure 1.

Contributions This paper describes two methods to improve color reproduction on digital cameras. Toward this goal, we first overview the current colorimetric mapping process and discuss why limitations in white balance create the need for per-illumination CSTs. Next, two methods for improving the colorimetric mapping are described. The first is to extend the current interpolation method to include an additional pre-calibrated illumination. This simple modification provides improved results and can be easily incorporated into the existing in-camera pipeline. Our second strategy requires no interpolation and uses a single fixed CST. This second method relies on true color constancy (i.e., full color balance) instead of traditional white balance and is currently suitable for use in an off-camera platform. Our experiments show that both proposed strategies offer notable improvements in the color reproduction accuracy for both DSLR and mobile phone cameras. As part of this work,

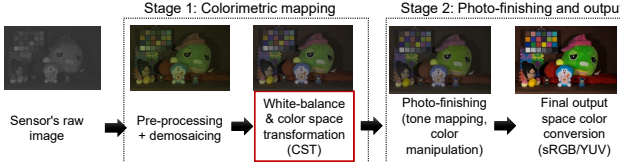


Figure 2: A diagram of a typical in-camera imaging pipeline. Work in this paper targets the colorimetric mapping in the first stage in this pipeline that converts the camera-specific color space to a perceptual color space. The procedure targeted by our work is highlighted in red and represents an intermediate step in the overall pipeline.

we have also created a dataset of 700 carefully calibrated colorimetric images for research in this area.

2. Motivation and related work

Motivation Before discussing related work, it is important to understand the motivation of our work and its context with respect to the in-camera pipeline. Figure 2 shows a standard diagram of the processing pipeline [33, 28]. At a high level, the overall pipeline can be categorized into two stages: (1) a colorimetric conversion and (2) photo-finishing manipulation. The first stage converts sensor RGB values from their camera-specific color space to a perceptual color space. The second stage involves a number of operations, such as tone and color manipulation, that modify the image’s appearance for aesthetic purposes.

Radiometric calibration methods (e.g., [8, 13, 14, 29, 40, 31]) target the reversal of the second stage to undo nonlinear processing for tasks such as photometric stereo and high-dynamic range imaging. Research on color reproduction applied on the camera—that is, the first stage in the pipeline—has seen significantly less attention. This is in part due to the lack of access to the camera hardware, since this first stage is applied onboard the camera. This restrictive access was addressed recently by Karaimer and Brown [28], who introduced a software-based camera emulator that works for a wide range of cameras. This software platform allows the pipeline to be stopped at intermediate steps and the intermediary pixel values to be accessed or modified. This platform has enabled the work performed in this paper, allowing the analysis of our proposed methods as well as the creation of an image dataset to evaluate the results.

In the following, we discuss two areas related to camera color reproduction: white balance and color calibration.

White balance and color constancy White balance (WB) is motivated by a more complex procedure, color constancy, that aims to make imaged colors invariant to a scene’s illumination. Computational color constancy is performed on cameras in order to mimic the human visual system’s ability to perceive objects as the same color under different illuminations [30]. Computational color constancy is a

two-step procedure: (1) estimate the scene illumination in the camera’s sensor color space; (2) apply a transform to remove the illumination’s color cast. Most color constancy research focuses only on the first step of illumination estimation. There is a wide range of approaches for illumination estimation, including statistical methods (e.g., [37, 21, 1]), gamut-based methods (e.g., [23, 15, 24]), and machine-learning methods (e.g., [2, 3, 11, 7]), including a number of recent approaches using convolutional neural networks (e.g., [27, 6, 35, 32]).

Once the illumination has been estimated, most prior work uses a simple 3×3 diagonal correction matrix that can be computed directly from the estimated illumination parameters. For most illuminations, this diagonal matrix guarantees only that neutral, or achromatic, scene materials (i.e., gray and white objects) are corrected [10]. As a result, this type of correction is referred to as “white balance” instead of color balance. Because WB corrects only neutral colors, the CST that is applied after WB needs to change, depending on the WB applied, and thus the CST is *illumination-specific*. This will be discussed in further detail in Section 3.

There have been several works that address the shortcoming of the diagonal 3×3 WB correction. Work by Finlayson et al. [17, 18] proposed the use of a spectral sharpening transform in the form of a 3×3 full matrix that was applied to the camera-specific color space. The transformed color space allowed the subsequent 3×3 diagonal WB correction to perform better. To establish the sharpening matrix, it was necessary to image known spectral materials under different illuminations. Chong et al. [12] later extended this idea to directly solve for the sharpening matrix by using the spectral sensitivities of the sensor. When the estimated sharpening matrix is combined with the diagonal matrix, these methods are effectively performing a full color balance. The drawback of these methods, however, is the need to have knowledge of the spectral sensitivities of the underlying sensor or imaged materials.

Recent work by Cheng et al. [10] proposed a method to compute a full color-balance correction matrix without the need of any spectral information of the camera or scene. Their work found that when scenes were imaged under specific types of broadband illumination (e.g., sunlight), the diagonal WB correction was sufficient to achieve full color balance. They proposed a method that allowed images under other illuminations to derive their full color correction using colors observed under broadband spectrum. This approach serves as the starting point for our second proposed method based on color balance instead of white balance.

Color calibration After white balance, a color space transform is applied to map the white-balanced raw image to a perceptual color space. Most previous work targeting color calibration finds a mapping directly between a cam-

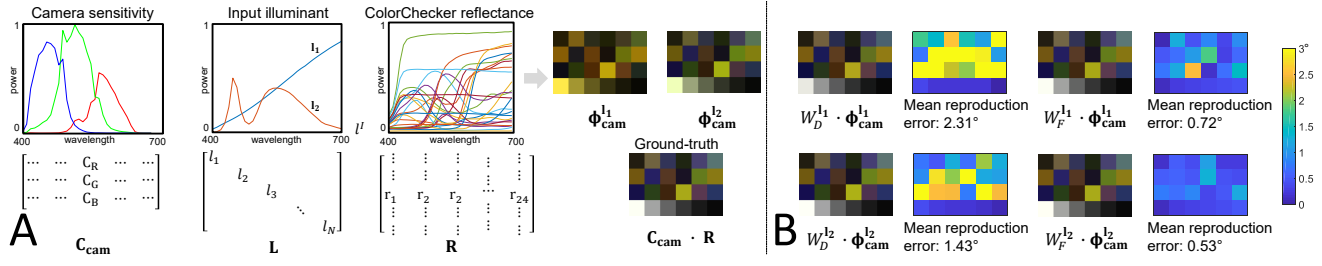


Figure 3: This figure is modeled after Cheng et al. [11]. (A) Image formation in the camera color space for two different illumination sources. (B) Result of a conventional diagonal WB (W_D) and full color correction (W_F) applied to the input images. Errors are computed as angular reproduction error (see Section 5.2). WB introduces notable errors for non-neutral colors. In addition, errors affect different scene materials depending on the illumination. Full color balance introduces fewer reproduction errors for all materials.

era’s raw-RGB values and a perceptual color space. Such color calibration is generally achieved by imaging a color rendition chart composed of color patches with known CIE XYZ values. Notable methods include Funt and Bastani [4] and Finlayson et al. [16, 19], who proposed a color calibration technique that eliminated the dependence on the scene intensities to handle cases where the color pattern was not uniformly illuminated. Hong et al. [26] introduced a color space transform based on higher-order polynomial terms that provided better results than 3×3 transforms. Finlayson et al. [20] recently proposed an elegant improvement on the polynomial color correction by using a fractional (or root) polynomial that makes this high-order mapping invariant to camera exposure. Bianco et al.’s [5] is one of the few works that considered the white-balance process by weighting the color space transform estimation based on the probability distribution of the illumination estimation algorithm.

While the above methods are related to our overall goal of color reproduction, these methods rely on a color rendition chart imaged under the scene’s illumination to perform the colorimetric mapping. As a result, they compute a direct mapping between the sensor’s RGB values and a target perceptual color space without the need for illumination correction, or, in the case of [5], require knowledge of the error distributions of the white-balance algorithm. Our work restricts itself to the current pipeline’s two-step procedure involving a camera color space illumination correction followed by a color space transform.

3. Existing camera colorimetric mapping

In this section, we describe the current colorimetric mapping process applied on cameras. We begin by first providing preliminaries of the goal of the colorimetric mapping procedure and the limitations arising from white balance. This is followed by a description of the current interpolation-based method used on cameras.

3.1. Preliminaries

Goal of the colorimetric mapping Following the notation of Cheng et al. [10], we model image formation using matrix notation. Specifically, let \mathbf{C}_{cam} represent a camera’s spectral sensitivity as a $3 \times N$ matrix, where N is the number of spectral samples in the visible range (400nm to 700nm). The rows of the matrix $\mathbf{C}_{\text{cam}} = [\mathbf{c}_R; \mathbf{c}_G; \mathbf{c}_B]^T$ correspond to the spectral sensitivities of the camera’s R, G, and B channels.

Since our work is focused on color manipulation, we can ignore the spatial location of the materials in the scene. As a result, we represent the scene’s materials as a matrix \mathbf{R} , where each matrix column, \mathbf{r}_i , is a $1 \times N$ vector representing the spectral reflectance of a material. Using this notation, the camera’s sensor responses to the scene materials, Φ_{cam}^I , for a specific illumination, I , can be modeled as:

$$\Phi_{\text{cam}}^I = \mathbf{C}_{\text{cam}} \operatorname{diag}(I) \mathbf{R} = \mathbf{C}_{\text{cam}} \mathbf{L} \mathbf{R}, \quad (1)$$

where I is a $1 \times N$ vector representing the spectral illumination and the $\operatorname{diag}(\cdot)$ operator creates a $N \times N$ diagonal matrix from a vector (see Figure 3).

The goal of the colorimetric mapping of a camera is to have all the colors in the scene transformed to a perceptual color space. This target perceptual color space can be expressed as:

$$\Phi_{xyz} = \mathbf{C}_{xyz} \mathbf{R}, \quad (2)$$

where \mathbf{C}_{xyz} is defined similar to \mathbf{C}_{cam} but uses the perceptual CIE 1931 XYZ matching functions [25]. In addition, the effects of the illumination matrix \mathbf{L} are ignored by assuming the scene is captured under ideal white light—that is, all entries of I are equal to 1.

The colorimetric mapping problem therefore is to map the camera’s Φ_{cam}^I under a particular illumination I , to the target perceptual color space with the illumination corrected—that is, Φ_{xyz} .

Deficiencies in white balance As previously discussed, the colorimetric mapping on cameras is performed in two steps.

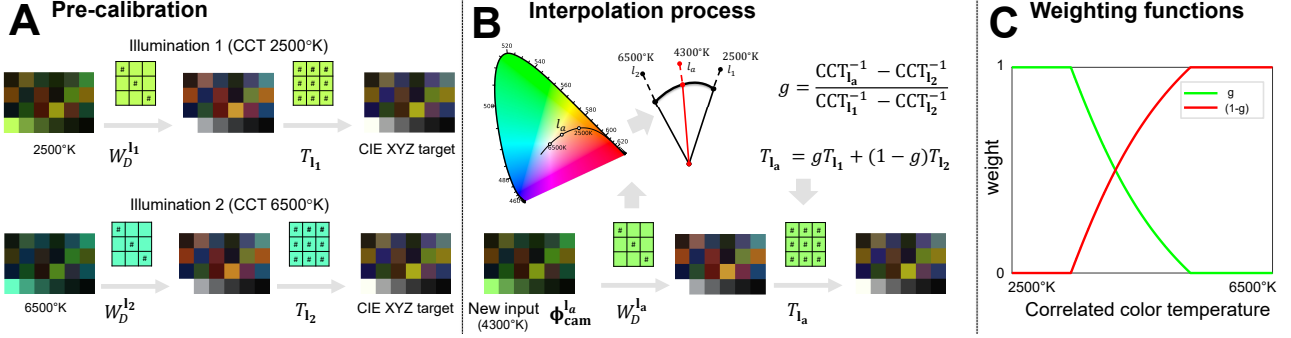


Figure 4: (A) Pre-calibration white-balance and CSTs for two illuminations with sufficiently different correlated color temperatures (CCT). (B) Interpolation procedure for an image captured under an arbitrary illumination. (C) A plot of the weights used to interpolate the new CST.

The first is to remove the effects of the illumination (i.e., computational color constancy) in the camera sensor’s color space. Ideally, computational color constancy estimates a 3×3 linear transform, W_F , to remove the illumination as follows:

$$W_F = \arg \min_{W_F} \| \mathbf{C}_{cam} \mathbf{R} - W_F \Phi_{cam}^1 \|^2, \quad (3)$$

where W_F minimizes the error between *all* the observed scene materials. Here the subscript F is used to denote that this matrix is a full 3×3 matrix.

However, most color constancy methods target only the estimation of the illumination in the camera space. This is equivalent to observing a neutral object in the scene (i.e., an achromatic material \mathbf{r} that reflects spectral energy at every wavelength equally) and thus $\mathbf{r} = \mathbf{l}$. The matrix to correct neutral patches can be derived directly from the observed illumination $\mathbf{C}_{cam} \mathbf{l}$ as:

$$W_D = \text{diag}(\mathbf{C}_{cam} \mathbf{l})^{-1}, \quad (4)$$

where \mathbf{l} is the observed scene illumination. The subscript D denotes that W_D is restricted to a diagonal 3×3 matrix. It should be clear that this diagonal white-balance correction is not the same as the full color correction formulation in Eq. (3).

The obvious drawback to WB is that it cannot guarantee that non-neutral scene materials are properly corrected. Moreover, errors in the non-neutral scene materials are dependant on the scene illumination. Figure 3 shows an example where the scene materials \mathbf{R} are the spectral properties of color patches from a standard color rendition chart. In this figure, the results of using the full color balance matrix W_F and the white-balance matrix, W_D , are applied to two different illuminations \mathbf{l}_1 and \mathbf{l}_2 . The errors are plotted as:

$$\begin{aligned} \text{Err}_{W_F^{l_i}} &= \| \mathbf{C}_{cam} \mathbf{R} - W_F^{l_i} \Phi_{cam}^{l_i} \|^2 \\ \text{Err}_{W_D^{l_i}} &= \| \mathbf{C}_{cam} \mathbf{R} - W_D^{l_i} \Phi_{cam}^{l_i} \|^2, \end{aligned} \quad (5)$$

where the index i is used to denote the different illuminations \mathbf{l}_1 or \mathbf{l}_2 . In this figure, the $W_F^{l_i}$ and $W_D^{l_i}$ are computed for the respective illuminations \mathbf{l}_i . We can see that the diagonal matrix incurs notable errors for non-neutral materials. These errors must be considered when computing the subsequent color space transform.

Color space transform (CST) Once the white-balance step has been applied, we now need to perform a mapping that considers the differences in the camera sensitivities \mathbf{C}_{cam} and the desired perceptual color space \mathbf{C}_{xyz} . Because the camera sensitivities of the sensor are generally unknown, it is common to derive this transform by imaging an object with known CIE XYZ values, most commonly a color rendition chart.

Working from Eq. (1), we assume the matrix \mathbf{R} is the spectral properties of the color rendition chart’s patches. Our goal is to compute a 3×3 CST matrix, T_l , that minimizes the following:

$$T_l = \arg \min_{T_l} \| \mathbf{C}_{xyz} \mathbf{R} - T_l W_D^l \Phi_{cam}^l \|^2, \quad (6)$$

where W_D^l is the estimated white-balance correction for the given illumination \mathbf{l} . Since the results of $W_D^l \Phi_{cam}^l$ differ depending on illumination, the matrix T_l needs to be estimated *per illumination* to compensate for the differences.

3.2. Current interpolation approach

Instead of computing a T_l per illumination, the current procedure used on cameras is to interpolate a CST based on two pre-calibrated illuminations. Figure 4 provides a diagram of the overall procedure. The two illuminations are selected such that their correlated color temperatures (CCT) are sufficiently far apart. For each illumination, the illumination-specific CST is estimated as shown in Figure 4-(A).

When an image is captured, its estimated illumination value is used to compute the correlated color temperature

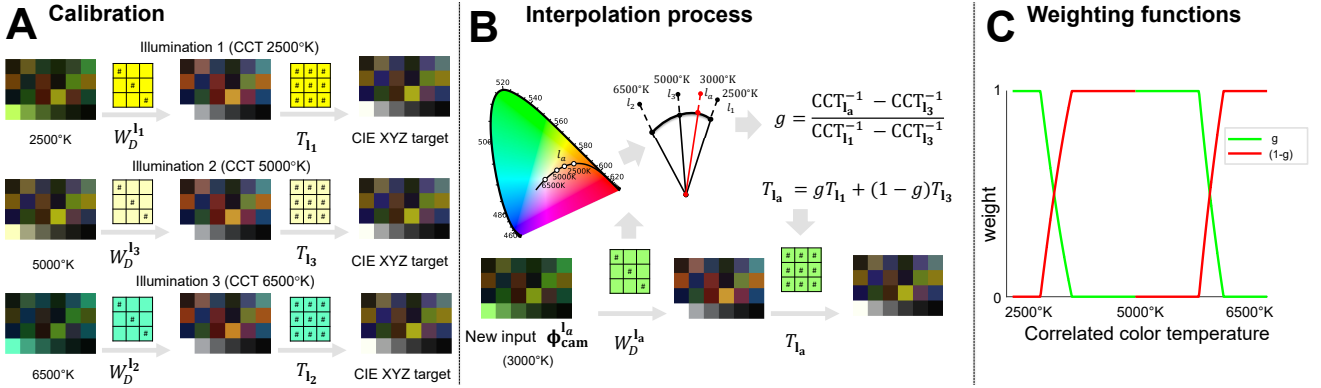


Figure 5: Our first method to improve the colorimetric mapping in the in-camera processing pipeline. (A) An additional illumination is calibrated and added to the interpolation process. (B) Shows the overall procedure to compute the weights to interpolate the CST. (C) Shows the weighting function for different estimated CCTs.

of the illumination [38, 34]. Based on the correlated color temperature, the two pre-computed CSTs are interpolated (see Figure 4-(B)) to obtain the final CST to be applied as follows:

$$T_1 = g T_{l_1} + (1 - g) T_{l_2}, \quad (7)$$

where

$$g = \frac{\text{CCT}_{l_1}^{-1} - \text{CCT}_{l_2}^{-1}}{\text{CCT}_{l_1}^{-1} - \text{CCT}_{l_3}^{-1}}. \quad (8)$$

The factory pre-calibrated CCTs for l_1 and l_2 for most cameras are selected to be 2500°K and 6500°K. The interpolation weights of g and $1 - g$ are shown in Figure 4-(C), where the horizontal axis is the CCT of the image's estimated illumination.

As shown in Figure 1, this interpolation procedure based on two fixed illuminations does not always provide good results. In the following sections, we describe two methods to improve the colorimetric mapping process.

4. Proposed improvements

We introduce two methods to improve the colorimetric mapping procedure. The first approach is a simple extension of the interpolation method to include an additional calibrated illumination in the interpolation process. The second method relies on a full color correction matrix discussed in Section 3.1 and uses a fixed CST matrix for all input images.

Method 1: Extending interpolation The most obvious way to improve the current colorimetric mapping procedure is to incorporate additional calibrated illuminations into the interpolation process. Ideally we would like many illuminations to be represented as control points in this process; however, this is likely unrealistic in a factory pre-calibration setting. As a result, we consider the case of adding only a single additional interpolation control point with a CCT at

approximately 5000°K. Figure 5-(A) shows a diagram of our approach.

When a new image is obtained, we estimate the scene illumination and then select which pair of pre-calibrated T_1 based on the estimated illumination's CCT. The blending weights g and $1 - g$ are adjusted accordingly between the pair of T selected using Eq. (8). The final CST, T_1 , is computed using Eq. (7). An example of this approach is shown in Figure 5-(B). The weighting factors for g are shown in Figure 5-(C). This simple inclusion of a single additional pre-calibrated illumination in the interpolation process gives surprisingly good results and can be readily incorporated into an existing in-camera pipeline.

Method 2: Using full color balance As discussed in Section 2, our second method leverages the full color-balance approach proposed by Cheng et al. [10]. A brief overview of the approach is provided here.

Cheng et al. [10] found that under certain types of broadband illumination, a diagonal correction matrix was sufficient to correct all colors in the camera's color space. Based on this finding, they proposed a method that first estimated a set of ground truth color values in the camera's sensor space by imaging a colorful object under broadband illumination (e.g., sunlight). This image is then corrected using a diagonal WB. Images of the same object under different illuminations could then map their observed colors to these ground truth camera-specific colors. The benefit of this approach is that unlike traditional color calibration, this approach *does not* require a color rendition chart with known CIE XYZ values; instead, any color pattern will work. Consequently, this approach falls short of colorimetric calibration, but does allow full color balance to be achieved.

Cheng et al. [10] also proposed a machine-learning approach that trained a Bayesian classifier to estimate the full color balance matrix, W_F^1 , for a given camera image Φ_{cam}^1

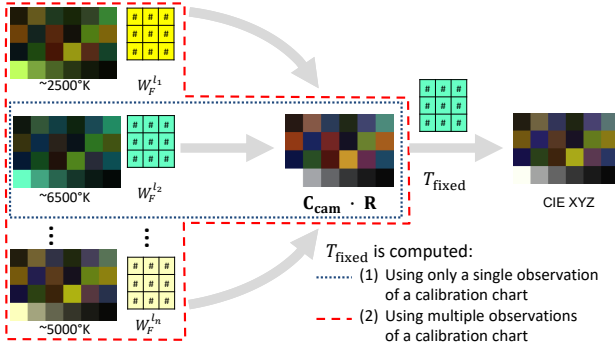


Figure 6: Our second method relies on full color balance matrices estimated using Cheng et al.’s [10] approach. A fixed CST is estimated using either a single observation of a calibration pattern or multiple observations.

under an arbitrary illumination \mathbf{l} . Since the full color balance attempts to correct all colors, it is not necessary to compute an illumination-specific CST. Instead, we can estimate a single *fixed* CST, T_{fixed} as follows:

$$T_{\text{fixed}} = \arg \min_T \left\| \sum_i (\mathbf{C}_{\text{xyz}} \mathbf{R} - T W_F^{\mathbf{l}_i} \Phi_{\text{cam}}^{\mathbf{l}_i}) \right\|^2, \quad (9)$$

where the index i selects an image in the dataset, \mathbf{l}_i represents the illumination for that image’s scene, and \mathbf{R} is again assumed to be calibration chart patches’ spectral responses.

In our second approach, we assume that the full color balance matrix can be obtained. We estimate the fixed CST, T_{fixed} , in two ways. The first is to use only a single observation of the color chart. Therefore Eq. (9) can be simplified such that i indexes to only a *single* observation of the color chart with a single illumination (we use an image with CCT of 6500°K). The second approach is to consider all observations of the color chart for each different illumination. Figure 6 provides an illustration of these two methods to estimate T_{fixed} . In our experiments, we distinguish the results obtained with these two different approaches.

Method 2 (extension): Full color balance with interpolation While the full color balance allows the computation of a fixed CST that should be applicable to all illuminations, from Eq. 9, it is clear the errors for the estimated CST mapping will be minimized for a particular illumination when only a single i is used as described above. As a result, we can use the same interpolation strategy as described in Sec. 3.2 that used WB corrected images, but instead use full color balance and CST estimated using Eq. 9. Results for this extension approach are not included in the main paper, but can be found in the accompanying supplemental materials.



Figure 7: Sample images from our dataset, including selected images from the publicly available NUS dataset [9] together with our mobile phone camera images.

5. Experimental results

In this section, our experimental setup used to test the proposed colorimetric mapping methods is discussed along with an evaluation of the proposed methods.

5.1. Setup and ground truth dataset

Our dataset consists of four DSLR cameras (Canon 1D, Nikon D40, Sony α 57, and Olympus E-PL6) and three mobile phone cameras (Apple iPhone 7, Google Pixel, and LG G4). For each camera we generate 100 colorimetrically calibrated images. For the DSLR cameras, we selected images from the NUS dataset [9] for calibration. The NUS dataset was created for research targeting color constancy and provides only ground truth for the illumination. This dataset has over 200 images per camera, where each camera is imaging the same scene. We select a subset of this dataset, considering images in which the color chart is sufficiently close to the camera and fronto-parallel with the respect to the image plane. For the mobile phone cameras, we captured our own images, taking scenes outdoors and in an indoor laboratory setting with multiple illumination sources. All scenes contained a color rendition chart. Like the NUS dataset, our dataset also carefully positioned the cameras such that they were imaging the same scene. Figure 7 shows an example of some of the images from our dataset.

Colorimetric calibration for each image in the dataset is performed using the X-Rite’s camera calibration software [39] that produces an image-specific color profile for each image. The X-Rite software computes a scene-specific white-balance correction and CST for the input scene. This is equivalent to estimating Eq. (4) and Eq. (6) based on CIE XYZ values of the X-Rite chart.

To obtain the colorimetrically calibrated image values, we used the software platform [28] with the X-Rite calibrated color profiles to process the images. The camera pipeline is stopped after the colorimetric calibration stage, as discussed in Section 2. This allows us to obtain the image at the colorimetric conversion stage *without* photo-finishing applied as shown in Figure 2.

Note that while the discussion in Section 3.1 used CIE

Method	Apple iPhone 7		Google Pixel		LG-G4		Canon1D		NikonD40		Sony α57		Olympus E-PL6	
	CC	I	CC	I	CC	I	CC	I	CC	I	CC	I	CC	I
CB + Fixed CST (all)	0.80	0.91	0.88	1.05	0.81	0.86	0.84	0.63	0.93	0.77	1.00	0.77	0.85	0.69
CB + Fixed CST (single)	0.95	1.04	1.41	1.45	1.17	1.17	0.95	0.76	0.98	0.80	0.99	0.76	0.82	0.67
WB + 3 CSTs	1.36	1.08	1.27	1.04	1.55	1.24	1.04	0.70	1.07	0.65	1.04	0.74	0.86	0.61
WB + 2 CSTs (re-calibrated)	1.76	1.42	1.92	1.46	1.98	1.54	1.16	0.82	1.33	0.82	1.13	0.81	1.05	0.71
WB + 2 CSTs (factory)	3.07	2.46	2.28	1.75	2.74	2.04	1.58	1.18	2.02	1.26	1.14	0.79	1.12	0.75

Table 1: The table shows the comparisons of error between full color balance with fixed CST, diagonal matrix correction with using three CST, native cameras (re-calibrated for the datasets we use), and native cameras (factory calibration). Errors are computed on color chart colors only (denoted as CC), and on full images (denoted as I). The top performance is indicated in bold and green. The second best method is in blue.

XYZ as the target perceptual color space, cameras instead use the Reference Output Medium Metric (ROMM) [36] color space, also known as ProPhoto RGB. ProPhoto RGB is a wide-gamut color space that is related to CIE 1931 XYZ by a linear transform. For our ground truth images, we stopped the camera pipeline after the values were transformed to linear-ProPhoto RGB color space. Thus, our 700-image dataset provides images in their unprocessed raw-RGB color space and their corresponding colorimetric calibrated color space in ProPhoto RGB.

5.2. Evaluation

We compare three approaches: (1) the existing interpolation method based on two calibrated illuminations currently used on cameras; (2) our proposed method 1 using interpolation based on three calibrated illuminations; (3) our proposed method 2 using the full color balance and a fixed CST.

The approach currently used on cameras is performed in two manners. First, we directly use the camera’s factory calibration of the two fixed CSTs. This can be obtained directly from the metadata in the raw files saved by the camera. To provide a fairer comparison, we use the X-Rite software to build a custom camera color profile using images taken from the dataset. Specifically, the X-Rite software provides support to generate a camera profile that replaces the factory default CST matrices. This color profile behaves exactly like the method described in Section 3. To calibrate the CSTs, we select two images under different illuminations (approximately 2500°K and 6500°K) from the dataset and use them to build the color space profile.

We then use the same 2500°K and 6500°K images to calibrate the CSTs used by our proposed method 1. We add an additional image with a CCT of approximately 5000°K as the third illumination. For the interpolation-based methods, we estimate the illumination in the scene using the color rendition chart’s white patches. This avoids any errors that may occur due to improper illuminant estimation. Similarly, for our method 2 that relies on full color balance, we compute the direct full color-balance matrix for a given input method based on the approach proposed by Cheng et al. [10]. This can be considered Cheng et al.’s method pro-

viding optimal performance.

Since each image in our dataset has a color rendition chart, errors are reported on the entire image as well as the color patches in the rendition chart. Moreover, since the different approaches (i.e., ground truth calibration and our evaluated methods) may introduce scale modifications in their respective mappings that affect the overall magnitude of RGB values, we do not report absolute RGB pixel errors, but instead report angular reproduction error [22]. This error can be expressed as:

$$\epsilon_r = \cos^{-1} \left(\frac{w^r \cdot w^{gt}}{\|w^r\| \|w^{gt}\|} \right), \quad (10)$$

where w^r is a linear-ProPhoto RGB value expressed as a vector produced by one of the methods and w^{gt} is its corresponding ground truth linear-ProPhoto RGB value also expressed as a vector.

Individual camera accuracy Table 1 shows the overall results for each camera and approaches used. The approaches are labeled as follows. CB+fixed CST refers to our method 2, using full color balance followed by a fixed CST. The (all) and (single) refer to the estimation of whether the CST uses either all images, or a single image as described in Section 4. WB+3 CSTs refers to our method 1 using an additional calibrated illumination. WB+2 CSTs refers to the current camera approach, where (recalibrated) indicates this approach is using the X-Rite color profile described above and (factory) indicates the camera’s native CST.

The columns show the different errors computed: (CC) is color chart patches errors only, and (I) for full images. The overall mean angular color reproduction error is reported. We can see that for all approaches our method 2 based on full color balance generally performs the best. Our method 1 performs slightly better in a few cases. The best improvements are gained from the mobile phone cameras; however, DSLRs do show a notable improvement as well.

Figure 8 shows visual results on whole images for two representative cameras, the LG-G4 and the Canon 1D. These results are accompanied by heat maps to reveal which parts of the images are being most affected by errors.

Method	Mobile Phones 2900°K	Mobile Phones 4500°K	Mobile Phones 5500°K	Mobile Phones 6000°K	DSLRs 3000°K	DSLRs 3500°K	DSLRs 4300°K	DSLRs 5200°K
CB + Fixed CST (all)	4.6	2.1	1.1	1.0	1.6	1.8	1.2	1.1
CB + Fixed CST (single)	10.0	7.1	4.9	6.2	2.7	2.9	2.1	1.7
WB + 3 CSTs	37.9	6.9	6.6	8.1	4.4	2.8	2.3	2.1
WB + 2 CSTs (re-calibrated)	44.9	11.3	9.5	16.7	6.7	3.2	3.4	5.9
WB + 2 CSTs (factory)	34.2	38.2	32.6	36.2	13.3	7.1	7.1	7.7

Table 2: This table reproduces the mean variance for color reproduction (in ProPhoto RGB chromaticity space) for mobile phone cameras and DSLR cameras of the 24 color patches on a color rendition chart. Results are shown for different scenes captured under different color temperatures. A lower variance means the color reproduction is more consistent among the cameras. (Variances values are $\times 1.0\text{E-}3$.) The top performance is indicated in bold and green. The second best method is in blue.

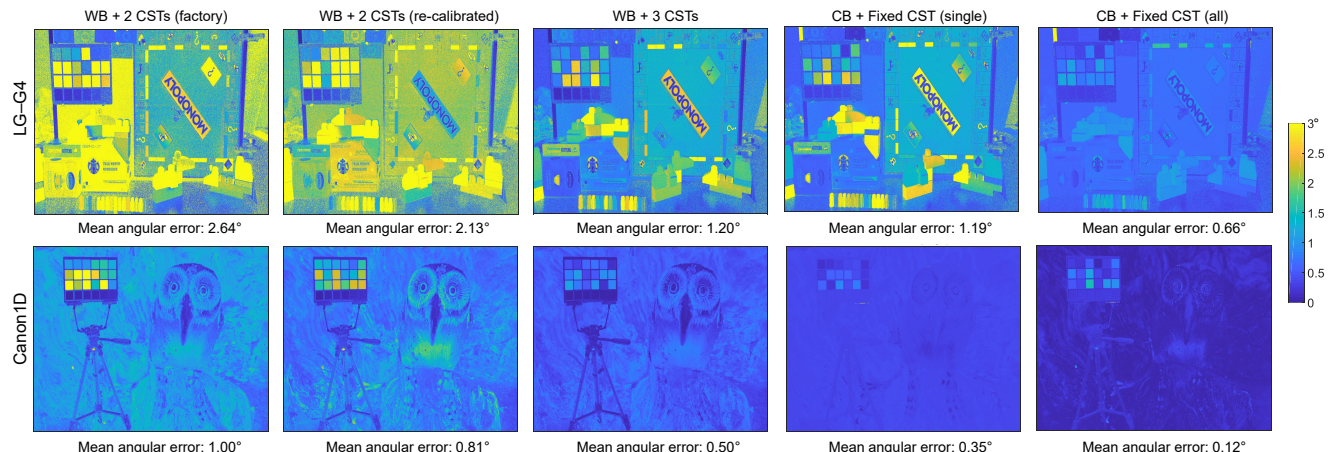


Figure 8: Visual comparison for the LG-G4 and Canon-1D. Methods used are the same as used for Table 2.

Multi-camera consistency One of the key benefits to improved colorimetric conversion is that cameras of different makes and models will capture scene colors in a more consistent manner. We demonstrate the gains made by our proposed approach by examining the reproduction of the color rendition chart patches among multiple cameras. From the dataset images, we select images under four different illumination temperatures. We then map each image using the respective methods and compute the mean variance of the color chart patches between the various approaches. The variance is computed in chromaticity space to factor out changes in brightness among the different cameras. Table 2 shows the result of this experiment. Our two proposed methods offer the most consistent mapping of perceptual colors.

6. Discussion and summary

We have presented two methods that offer improvements for color reproduction accuracy for cameras. Our first method expands the current interpolation procedure to use three fixed illumination settings. This simple modification offers improvements up to 19% (DSLR cameras) and

33% (mobile phone cameras); moreover it can be easily incorporated into existing pipelines with minimal modifications and overhead. Our second method leverages recent work [10] that allows full color balance to be performed in lieu of white balance. This second method provides the best overall color reproduction, with improvements up to 30% (DSLR cameras) and 59% (mobile phone cameras). This work by [10] requires a machine-learning method to predict the color balance matrix. Because most cameras still rely on fast statistical-based white-balance methods, our second proposed method is not yet suitable for use onboard a camera, but can be beneficial to images processed off-line. These results, however, suggest that future generations of camera designs would benefit from exploiting advances offered by machine-learning methods as part of the color reproduction pipeline.

Acknowledgments This study was funded in part by a Google Faculty Research Award, the Canada First Research Excellence Fund for the Vision: Science to Applications (VISTA) programme, and an NSERC Discovery Grant. We thank Michael Stewart for his effort in collecting our mobile phone dataset.

References

- [1] K. Barnard, V. Cardei, and B. Funt. A comparison of computational color constancy algorithms. i: methodology and experiments with synthesized data. *IEEE Transactions on Image Processing*, 11(9):972–984, 2002.
- [2] J. T. Barron. Convolutional color constancy. In *ICCV*, 2015.
- [3] J. T. Barron and Y.-T. Tsai. Fast Fourier color constancy. In *CVPR*, 2017.
- [4] P. Bastani and B. Funt. Simplifying irradiance independent color calibration. In *Color and Imaging Conference*, 2014.
- [5] S. Bianco, A. Bruna, F. Naccari, and R. Schettini. Color space transformations for digital photography exploiting information about the illuminant estimation process. *Journal of Optical Society America A*, 29(3):374–384, 2012.
- [6] S. Bianco, C. Cusano, and R. Schettini. Single and multiple illuminant estimation using convolutional neural networks. *IEEE Transactions on Image Processing*, 26(9):4347–4362, 2017.
- [7] A. Chakrabarti. Color constancy by learning to predict chromaticity from luminance. In *NIPS*, 2015.
- [8] A. Chakrabarti, D. Scharstein, and T. Zickler. An empirical camera model for internet color vision. In *BMVC*, 2009.
- [9] D. Cheng, D. K. Prasad, and M. S. Brown. Illuminant estimation for color constancy: why spatial-domain methods work and the role of the color distribution. *Journal of Optical Society America A*, 31(5):1049–1058, 2014.
- [10] D. Cheng, B. Price, S. Cohen, and M. S. Brown. Beyond white: ground truth colors for color constancy correction. In *ICCV*, 2015.
- [11] D. Cheng, B. Price, S. Cohen, and M. S. Brown. Effective learning-based illuminant estimation using simple features. In *CVPR*, 2015.
- [12] H. Y. Chong, S. J. Gortler, and T. Zickler. The von Kries hypothesis and a basis for color constancy. In *ICCV*, 2007.
- [13] P. E. Debevec and J. Malik. Recovering high dynamic range radiance maps from photographs. In *SIGGRAPH*, 1997.
- [14] M. Diaz and P. Sturm. Radiometric calibration using photo collections. In *ICCP*, 2011.
- [15] G. D. Finlayson. Color in perspective. *IEEE Transactions on Pattern Analysis and Machine Intelligence*, 18(10):1034–1038, 1996.
- [16] G. D. Finlayson, M. M. Darrodi, and M. Mackiewicz. The alternating least squares technique for nonuniform intensity color correction. *Color Research & Application*, 40(3):232–242, 2015.
- [17] G. D. Finlayson, M. S. Drew, and B. V. Funt. Color constancy: enhancing von Kries adaption via sensor transformations. In *Human Vision, Visual Processing and Digital Display IV*, 1993.
- [18] G. D. Finlayson, M. S. Drew, and B. V. Funt. Diagonal transforms suffice for color constancy. In *ICCV*, 1993.
- [19] G. D. Finlayson, H. Gong, and R. B. Fisher. Color homography color correction. In *Color and Imaging Conference*, 2016.
- [20] G. D. Finlayson, M. Mackiewicz, and A. Hurlbert. Color correction using root-polynomial regression. *IEEE Transactions on Image Processing*, 24(5):1460–1470, 2015.
- [21] G. D. Finlayson and E. Trezzi. Shades of gray and color constancy. In *Color and Imaging Conference*, 2004.
- [22] G. D. Finlayson, R. Zakizadeh, and A. Gijsenij. The reproduction angular error for evaluating the performance of illuminant estimation algorithms. *IEEE Transactions on Pattern Analysis and Machine Intelligence*, 39(7):1482–1488, 2017.
- [23] D. A. Forsyth. A novel algorithm for color constancy. *International Journal of Computer Vision*, 5(1):5–35, 1990.
- [24] A. Gijsenij, T. Gevers, and J. van de Weijer. Generalized gamut mapping using image derivative structures for color constancy. *International Journal of Computer Vision*, 86(2):127–139, 2010.
- [25] J. Guild. The colorimetric properties of the spectrum. *Philosophical Transactions of the Royal Society of London*, 230:149–187, 1932.
- [26] G. Hong, M. R. Luo, and P. A. Rhodes. A study of digital camera colorimetric characterisation based on polynomial modelling. *Color Research & Application*, 26(1):7684, 2001.
- [27] Y. Hu, B. Wang, and S. Lin. Fc 4: Fully convolutional color constancy with confidence-weighted pooling. In *CVPR*, 2017.
- [28] H. C. Karaimer and M. S. Brown. A software platform for manipulating the camera imaging pipeline. In *ECCV*, 2016.
- [29] S. J. Kim, H. T. Lin, Z. Lu, S. Susstrunk, S. Lin, and M. S. Brown. A new in-camera imaging model for color computer vision and its application. *IEEE Transactions on Pattern Analysis and Machine Intelligence*, 34(12):2289–2302, 2012.

- [30] J. J. McCann, S. P. McKee, and T. H. Taylor. Quantitative studies in retinex theory a comparison between theoretical predictions and observer responses to the “color mondrian” experiments. *Vision Research*, 16(5):445–458, 1976.
- [31] R. M. Nguyen and M. S. Brown. Raw image reconstruction using a self-contained srgb-jpeg image with only 64 kb overhead. In *CVPR*, 2016.
- [32] S. W. Oh and S. J. Kim. Approaching the computational color constancy as a classification problem through deep learning. *Pattern Recognition*, 61:405–416, 2017.
- [33] R. Ramanath, W. E. Snyder, Y. Yoo, and M. S. Drew. Color image processing pipeline. *IEEE Signal Processing Magazine*, 22(1):34–43, 2005.
- [34] A. R. Robertson. Computation of correlated color temperature and distribution temperature. *Journal of Optical Society America*, 58(11):1528–1535, 1968.
- [35] W. Shi, C. C. Loy, and X. Tang. Deep specialized network for illuminant estimation. In *ECCV*, 2016.
- [36] K. E. Spaulding, E. Giorgianni, and G. Wolfe. Reference input/output medium metric rgb color encodings (rimm/romm rgb). In *Image Processing, Image Quality, Image Capture, Systems Conference*, 2000.
- [37] J. van de Weijer, T. Gevers, and A. Gijsenij. Edge-based color constancy. *IEEE Transactions on Image Processing*, 16(9):2207–2214, 2007.
- [38] G. Wyszecki and W. S. Stiles. *Color science (2nd Edition)*. Wiley, 2000.
- [39] X-Rite Incorporated. *ColorChecker Camera Calibration (Version 1.1.1)*, accessed March 28, 2018. http://xritephoto.com/ph_product_overview.aspx?ID=1257&Action=Support&SoftwareID=1806.
- [40] Y. Xiong, K. Saenko, T. Darrell, and T. Zickler. From pixels to physics: Probabilistic color de-rendering. In *CVPR*, 2012.